

# Development of a Graphene-Oxide-Deposited Carbon Electrode for the Rapid and Low-Level Detection of Fentanyl and Derivatives

Daniel Jun, Glenn Sammis, Pouya Rezazadeh-Azar, Erwann Ginoux, and Dan Bizzotto\*

Cite This: *Anal. Chem.* 2022, 94, 12706–12714

Read Online

ACCESS |



Metrics &amp; More

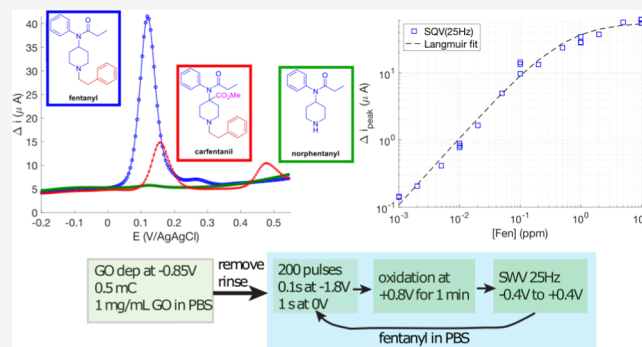


Article Recommendations



Supporting Information

**ABSTRACT:** The opioid overdose crisis in North America worsened during the COVID-19 pandemic, with multiple jurisdictions reporting more deaths per day due to the fentanyl-contaminated drug supply than COVID-19. The rapid quantitative detection of fentanyl in the illicit opioid drug supply or in bodily fluids at biologically relevant concentrations (i.e., <80 nM) remains a significant challenge. Electroanalytical techniques are inexpensive and can be used to rapidly detect fentanyl, but detection limits need to be improved. Herein, we detail the development of an electrochemical-based fentanyl analytical detection strategy that used a glassy carbon electrode modified with electrochemically reduced graphene oxide (ERGO) via electrophoretic deposition. The resulting surface was further electrochemically reduced in the presence of fentanyl to enhance the sensitivity. Multiple ERGO thicknesses were prepared in order to prove the versatility and ability to fine-tune the layer to the desired response. Fentanyl was detected at <10 ppb (<30 nM) with a limit of detection of 2 ppb and a calibration curve that covered 4 orders of concentration (from 1 ppb to 10 ppm). This method was sensitive to fentanyl analogues such as carfentanil. Interference from the presence of 100-fold excess of other opioids (heroin, cocaine) or substances typically found in illicit drug samples (e.g. caffeine and sucrose) was not significant.



## INTRODUCTION

Canada and the United States are in the midst of a public health crisis. The number of overdoses and deaths caused by opioids, including fentanyl, has risen sharply and continues to rise. From January 2016 to September 2021, almost 27,000 lives were lost in Canada alone due to opioid overdoses, 86% of them involving fentanyl, and of these, most being accidental (>98%).<sup>1,2</sup> Coupled with the COVID-19 pandemic, the overdose crisis has become even more deadly as harm reduction and addiction services are increasingly difficult to access.<sup>3</sup> The huge increase from baseline overdose deaths (before 2015) related to opioid use is due to the substitution of heroin and/or cocaine in part or in whole by fentanyl (*N*-phenyl-*N*-[1-(2-phenylethyl)piperidin-4-yl]propanamide)<sup>4</sup> and/or its derivatives such as carfentanil<sup>5</sup> (Figure 1).

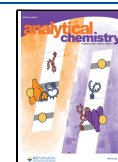
The high potency of fentanyl is not only a health challenge but it also poses a significant analytical challenge for detecting small amounts of opioids in illicit drug samples for harm mitigation strategies or in physiological fluids supporting effective clinical treatments of opioid use disorder.<sup>6</sup> The current techniques to detect fentanyl range from non-quantitative assessments to highly accurate lab-based analytical quantification. Fentanyl test strips produce a binary response that is highly sensitive to the presence of fentanyl and provides a rapid response within minutes, but due to the prevalence of and contamination by fentanyl in trace amounts, the result is

often not useful since a quantitative response is not generated. Liquid chromatography mass spectrometry can be used to identify and measure the concentration of opioids in drug samples and in human serum;<sup>7</sup> however, the turnaround time to process a sample in a centralized laboratory is long, and the procedure typically requires expensive equipment and specialized training of technicians; though advances toward portable MS have been published, they are not yet capable of point-of-use (POU) applications, which are needed to advance harm mitigation and drug treatment strategies.<sup>8</sup> Other techniques, such as surface-enhanced Raman spectroscopy and Fourier transform infrared (FTIR) spectroscopy, have been used previously and have their limitations in analyzing mixtures.<sup>9,10</sup> Liquid chromatography with electrochemical detection has been proven to be effective as most compounds of interest can be oxidized but as with MS are difficult to translate to POU devices.<sup>11–13</sup>

Received: May 11, 2022

Accepted: August 25, 2022

Published: September 9, 2022



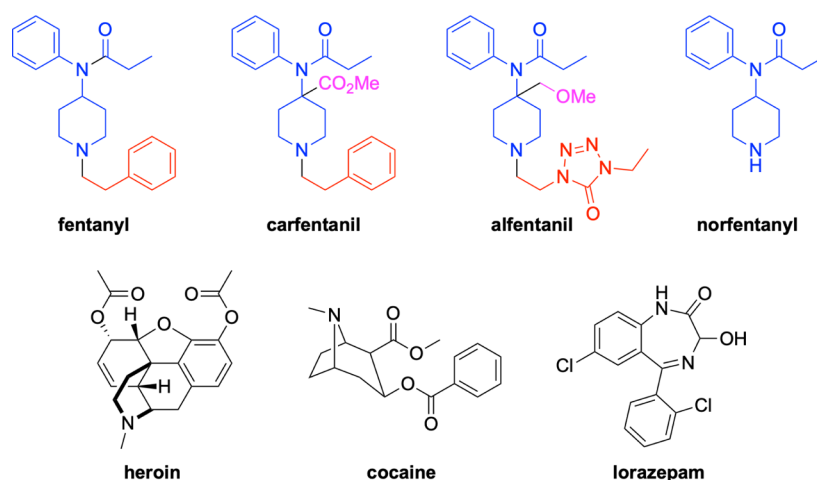


Figure 1. Chemical structures of many of the compounds used in this work.

POU electroanalytical devices offer the opportunity to quickly identify and quantify opioid species.<sup>14</sup> Electrochemical techniques are versatile and can be used on drug samples from the field or on bodily fluids of a patient for the purposes of treatment. Electroanalytical devices can be made to be inexpensive and portable as shown with many examples in the literature such as the implementation of a micro-catheter for continuous monitoring of fentanyl,<sup>15</sup> or with micro-needle sensor arrays,<sup>16</sup> or using modified disposable screen-printed electrodes.<sup>17,18</sup> A recent review of these electroanalytical approaches used to quantify fentanyl<sup>19</sup> highlighted the need to improve detector sensitivity to measure low-concentration contamination in street drugs or at physiologically relevant concentrations (80 nM or 30 ppb) and for the identification of common fentanyl analogues that are part of the illicit drug supply.

Herein, we show that using a glassy carbon (GC) electrode modified with graphene oxide (GO), electrochemical detection is rapid and highly sensitive (<10 ppb) to the presence of fentanyl and competitive with other electroanalytical approaches.<sup>17–21</sup> Furthermore, we have been able to identify and quantify fentanyl and fentanyl derivatives and in the presence of fillers or cutting agents or other opioids without requiring a chromatographic separation.

## MATERIALS AND METHODS

**Chemicals.** Aqueous solutions of phosphate-buffered saline (PBS) (1.8 mM  $\text{KH}_2\text{PO}_4$ , 10 mM  $\text{Na}_2\text{HPO}_4$ , 2.7 mM KCl, and 137 mM NaCl all from Fisher Scientific) pH 7.4 were prepared with Millipore Milli-Q ultrapure water (18.2 M $\Omega$  cm). The GO suspension (Graphenea, particle size < 10  $\mu\text{m}$ ) was diluted from 4 mg/mL to a final concentration of 1 mg/mL with PBS. Fentanyl, norfentanyl, alfentanil, carfentanil, lorazepam, heroin, and cocaine were all sourced as analytical standards (1 or 0.1 mg/mL in methanol or acetonitrile) from Sigma-Aldrich (Cerilliant), and caffeine and sucrose (from Sigma-Aldrich) were diluted to the required final concentration with PBS (structures are shown in Figure 1).

**Electrochemistry.** The electrochemical experiments were conducted in a glass cell in a three-electrode configuration with the GC working electrode (CHI104, 0.3 cm dia.), a Ag/AgCl reference electrode (BASi), and a platinum counter electrode connected to a potentiostat (Autolab PGSTAT12). All

solutions were deaerated with Ar to remove  $\text{O}_2$ . All potentials are with reference to Ag/AgCl.

Cyclic voltammetry (CV) measurements were typically performed at 100 mV/s. Square wave voltammetry (SWV) measurements were performed using a 5 mV step potential and a 20 mV amplitude at 25 Hz. Additional frequencies of 7 and 37 Hz were used. The positive going potential scans were analyzed using MATLAB. The peak currents were extracted after correcting for the background and fitting the SWV peaks to a Gaussian.

Electrochemical impedance spectroscopy (EIS) was performed at  $-0.1$  V to avoid possible interference with the fentanyl peak centered at 0.08 V. A 10 mV root-mean-square perturbation was applied over a frequency range from 1 Hz to 10 kHz. The impedance spectra were fit to one of two equivalent circuits (shown in Figure S1) that were composed of a solution resistance ( $R_{\text{soln}}$ ) in series with a parallel combination of a constant phase element (CPE) ( $Z_{\text{CPE}}$ ) and a series R and C representing the volumetric charging of the deposited GO (RC). The stray capacitance ( $C_{\text{stray}}$ ) was also part of the fitting, but this value (20–40 nF) did not fluctuate between samples and was characteristic of the measurement setup. The statistically relevant equivalent circuit ( $p = 0.05$ ) was determined using an  $F$  test following the literature.<sup>22</sup>

### Cleaning and Conditioning of the GC Electrode.

Before each use, the GC electrode was rinsed with Milli-Q water, polished on a nylon pad with a thin slurry of alumina (0.05  $\mu\text{m}$ , Metrohm), and thoroughly rinsed under a steady stream of Milli-Q water again. At the beginning of the day, prior to any electrochemical experiments, the electrode was placed into the PBS electrolyte, and a series of potential pulses were applied ( $-1.8$  V for 0.1 s, 0 V for 1 s, repeated 100 times) to condition the electrode.

**Electrophoretic Deposition and Reduction of GO.** The polished and conditioned GC electrode was immersed in a GO suspension (1 mg/mL) in PBS. The solution was deaerated with Ar to remove dissolved  $\text{O}_2$ . A single CV cycle (100 mV/s) from 0.1 to  $-0.8$  V was recorded using a Ag/AgCl reference electrode. Subsequently,  $-0.85$  V was applied until a fixed amount of charge ( $-0.25$ ,  $-0.5$ , and  $-1$  mC) was delivered to the electrode. Examples are provided in Figure S2. The currents were between 1 and 2  $\mu\text{A}$  over 200–400 s.

The electrophoretically deposited layers of GO were electrochemically reduced onto the GC electrode during

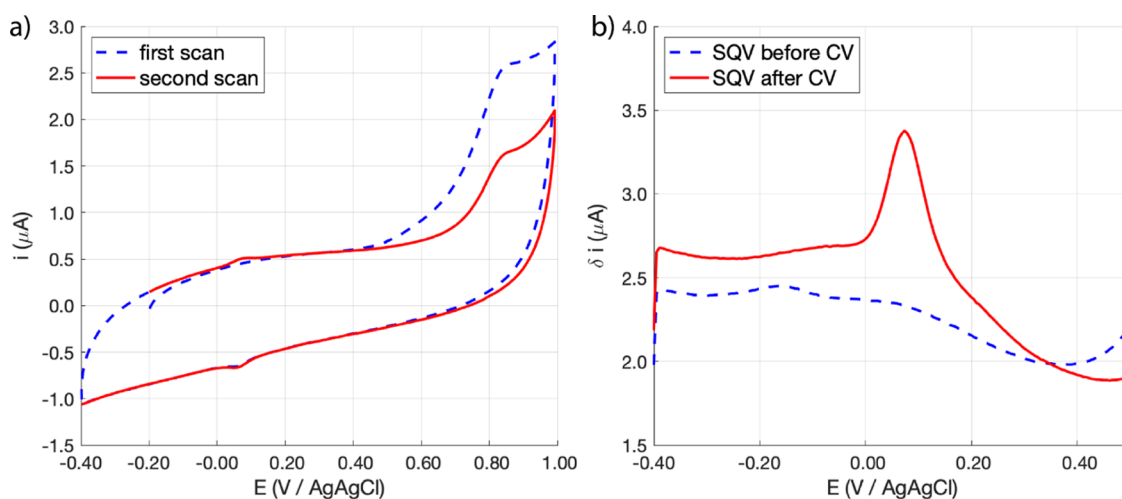


**Figure 2.** (a) Oxidation of fentanyl (1 ppm or 1 mg/mL) on GC. (a) CV (20 mV/s) and (b) SWV (25 Hz) of GC before (dashed line - - -) and after (solid line —) scanning to +1.0 V/AgAgCl in the presence of 1 ppm fentanyl.

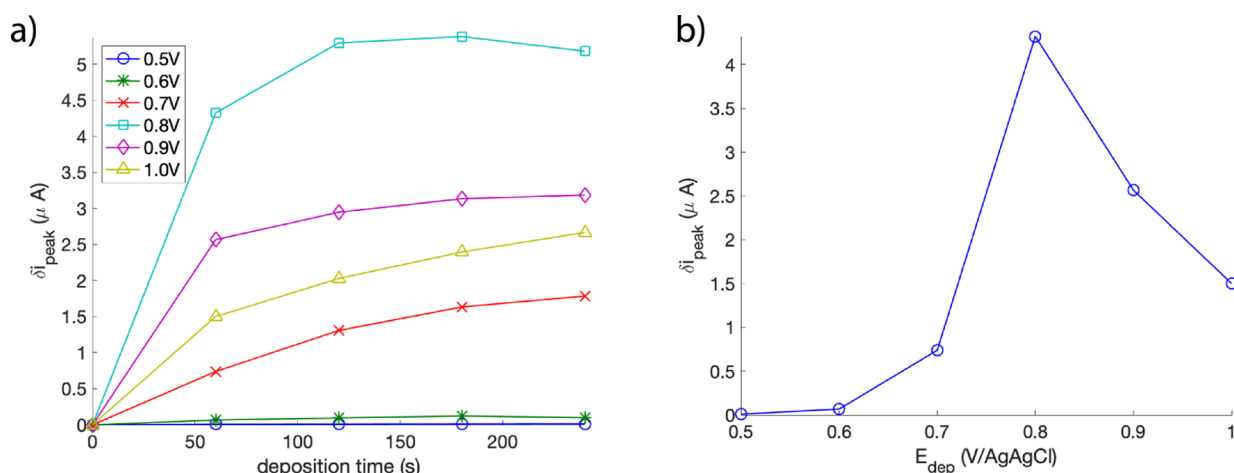


**Figure 3.** (a) SWV peak currents for the +0.08 V/AgAgCl redox process after applying a fixed potential for a total of 1, 2, 3, and 4 min. (b) SWV peak currents for the +0.08 V/AgAgCl peak after 1 min at the designated potential. The PBS electrolyte contained 1 ppm (1 mg/mL) fentanyl. SWV was measured at 25 Hz.

deposition at  $-0.85$  V, but as detailed previously,<sup>23,24</sup> reductive potential pulses were observed to improve the quality of the deposit. The modified electrode was placed into the PBS electrolyte (without or with fentanyl) and a series of potential pulses were applied ( $-1.8$  V for 0.1 s, 0 V for 1 s, typically repeated 200 times), while the solution was stirred.

**Electrochemical Analysis of Fentanyl and Fentanyl Derivatives.** Fentanyl and fentanyl derivatives were diluted from the analytical stock solutions with PBS to afford the final concentrations analyzed [ranging from 1 ppb (or 1  $\mu\text{g/mL}$ ) to 10 ppm (or 10  $\text{mg/mL}$ )]. A potential of +0.8 V (unless otherwise indicated) was applied for 1 min (or in 1 min increments for a total oxidation time of 4 min) to oxidize fentanyl while the solution was stirred. After each round of oxidation, SWV measurements were made as described above.

## RESULTS AND DISCUSSION

### Electrochemical Oxidation of Fentanyl on GC.

Fentanyl has an oxidative peak at +0.85 V on GC as can be seen in the cyclic voltammogram in Figure 2. Fentanyl analogues were also shown to oxidize at a similar potential.<sup>19</sup> The oxidation peak current has been used for quantification;

however, its usefulness is limited in more complex samples, such as mixtures consisting of other opioids (e.g., cocaine and heroin), due to their similar oxidative peak potentials (Figure S3). Oxidation of fentanyl at positive potentials resulted in the appearance of a new set of redox peaks at +0.08 V as previously reported.<sup>19,20</sup> Figure 2 confirms that the oxidation of fentanyl was necessary to produce the new redox features at +0.08 V corresponding to a byproduct of fentanyl oxidation. The oxidation at +0.8 V was proposed to be a de-alkylation of fentanyl to produce norfentanyl<sup>19</sup> thought to be the redox-active compound at +0.08 V. This hypothesis will be tested in our work. The oxidized fentanyl appeared to adsorb onto the electrode surface, which was confirmed since the peak currents were linear with an increasing CV scan rate (Figure S4).

SWV was used to measure the presence of adsorbed fentanyl oxidation products at +0.08 V. SWV allowed for a measurement with decreased background capacitance signals as compared to CV. The oxidized fentanyl redox peak is significantly far removed from the oxidation at higher potentials (+0.8 V) and facilitates a sensitive approach for the quantification of fentanyl, even in the presence of other opioids. This redox feature can be exploited for fentanyl

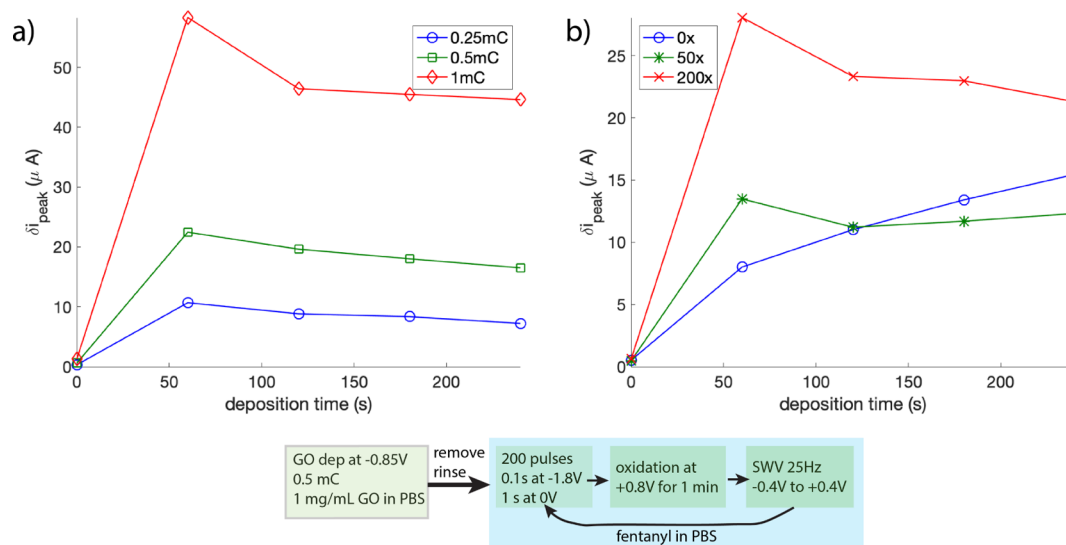


**Figure 4.** (a) SWV peak current from the oxidized fentanyl redox at  $+0.08$  V/AgAgCl for three different ERGO layers (increasing deposition charge) for increasing deposition time at  $+0.8$  V/AgAgCl. These layers were pre-treated using 200 reductive potential pulses in the presence of  $0.5$  ppm fentanyl. (b) SWV peak currents measured after pre-treatment with different numbers of reductive potential pulses for the  $0.5$  mC ERGO deposit in PBS with  $0.5$  ppm fentanyl for increasing deposition time at  $+0.8$  V/AgAgCl. A flowchart is provided outlining the workflow.

quantification using an oxidative adsorption strategy that enables accumulation on the electrode surface (pre-concentration step) prior to measurements using SWV.

To optimize the sensitivity of fentanyl detection, discrete oxidative potentials were used for a range of deposition times. The GC potential was held at discrete values, from  $+0.5$  to  $+1$  V at  $0.1$  V increments, for  $1$  min of oxidation and repeated for up to a total of  $4$  min of oxidation. After each minute at the constant potential, a SWV ( $-0.4$  to  $+0.4$  V) was measured, and the adsorbed oxidized fentanyl redox peak heights were determined (Figure 3). For each potential used to oxidize fentanyl, the majority of the signal was obtained after  $1$  min, with a minimal increase in signal and/or saturation was observed within  $4$  min. A significant potential dependence was noted with the optimum oxidative adsorption potential of  $+0.8$  V. Higher potentials, such as  $+0.9$  and  $+1$  V, resulted in a decrease in the fentanyl signal, which could be attributed to the oxidation of the carbon surface. The amount of oxidized fentanyl accumulated on the GC surface that remained for subsequent SWV analysis appeared to have had a potential dependence that correlated with the oxidation observed in CV, clearly indicating that the redox process at  $+0.08$  V required the oxidation of fentanyl at positive potentials. No measurable signal was obtained for oxidation at potentials below  $+0.5$  V.

The sensitivity of fentanyl analysis using a polished GC electrode was found to have a limited range (vide infra). Improvements in sensitivity can be achieved through modification of the electrode surface with carbon nanoparticles or graphene, which was demonstrated for fentanyl detection in particular.<sup>21</sup> To improve the analytical performance, the GC surface was modified with the electrophoretic deposition and reduction of GO following the procedures developed previously on a gold electrode.<sup>23,24</sup>

**Characterization of the Electrophoretic Deposition of GO Films on GC.** Following previously developed methods, GO was electrophoretically deposited and reduced on the GC electrode, producing an electrochemically reduced GO (ERGO) film. This work follows on from our previous studies depositing ERGO on gold electrodes and analyzing the ERGO

layers using Raman and assessing the overlayer conductivity through the use of metal electrodeposition.<sup>23,24</sup> We show that this approach was reproducible and consistent and offers an alternative to other methods of incorporating GO into electrochemical sensors.<sup>21</sup> The resulting layers were characterized by CV and EIS to determine the changes to the surface.

**Properties of GO Deposits.** Initially, three ERGO layers of differing thicknesses were characterized. The ERGO deposition was based on the total amount of charge passed at  $-0.85$  V, which were ordered from thinnest to thickest:  $0.25$ ,  $0.5$ , and  $1$  mC as shown by impedance measurements (EIS). EIS was performed at  $-0.1$  V to characterize the interface after deposition and after pulsing treatments (results shown in Figure S5 and Tables S1 and S2). After deposition, the capacitance of the interface increased with the deposition charge [the CPE increased from  $13.5$  ( $0.25$  mC),  $22$  ( $0.5$  mC), to  $37.7$  ( $1.0$  mC), all with the same exponent ( $0.9$ – $0.93$ )] showing the expected increase in surface area. The CPE exponent characterized the uniformity of the deposit which was close to  $1$  ( $0.91 \pm 0.01$ ) and did not show any dependence on the deposition charge. The surface therefore behaved like a capacitor with increasing surface area with deposition charge because of increased surface roughness but without significant porosity. As the rate of deposition did not change dramatically (Figure S2), the ERGO overlayer would have grown consistently with time, most likely resulting in the same kind of non-porous but rough surface.

The analytical performance of the ERGO deposits was evaluated. Following deposition, the ERGO layer was subsequently further reduced with a series of  $200$  potential pulses ( $-1.8$  V for  $0.1$  s and  $0$  V for  $1$  s) in the presence of  $0.5$  ppm fentanyl. The effects of pulsing on the ERGO layer will be described in the next section. This was followed by the oxidation for  $1$  min at  $+0.8$  V in the presence of  $0.5$  ppm fentanyl. The negative potential pulsing and  $+0.8$  V oxidation procedure was repeated for a total of  $4$  min of oxidation.

As can be seen in Figure 4a, the fentanyl signal increased with the thicker ERGO layer; an approximate doubling of the  $25$  Hz SWV peak current measured at  $+0.1$  V correlated with

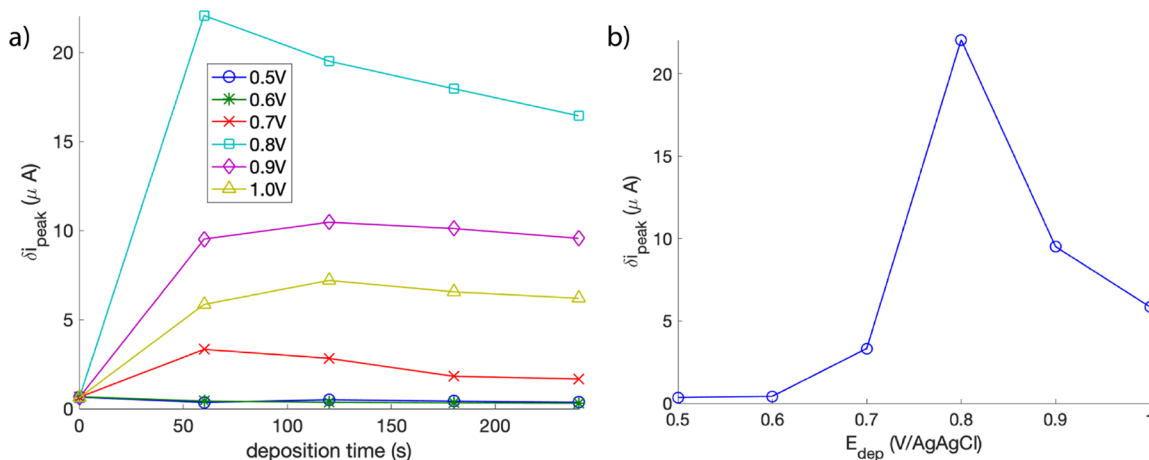


**Figure 5.** (a) SWV peak currents for the +0.08 V/AgAgCl redox process on a 0.5 mC ERGO-modified GC electrode conditioned by 200 negative potential pulses after applying a fixed potential for a total of 1, 2, 3, and 4 min. (b) SWV peak currents for the +0.08 V/AgAgCl peak after 1 min at the designated potential. The PBS electrolyte contained 0.5 ppm fentanyl. SWV was measured at 25 Hz.

the doubling of total ERGO deposition charge. The advantage of a thin 0.25 mC layer was that the signal-to-background current was superior to that of a thick 1 mC layer. A thicker layer has a larger background charging current due to larger area and capacitance, making low concentrations of fentanyl difficult to detect. Conversely, a thick 1 mC layer has a higher capacity and does not reach saturation as quickly as the thin 0.25 mC layer. Essentially, different thicknesses of ERGO can be created and fine-tuned for the desired analytical application, whether high sensitivity or high capacity is required. The 0.5 mC ERGO deposit was selected as having the optimal background with largest dynamic range for further use. Examples of the background and oxidized fentanyl signals at +0.1 V are shown in Figure S8 for GC, 0.5, and 1.0 mC ERGO deposits.

**Electrochemical Reductive Potential Pulsing of the Deposited ERGO Layer.** As demonstrated above, a number of reductive potential pulses were applied after the deposition of GO on GC because they were previously shown to anneal the carbon flakes of the GO together and create a more robust layer.<sup>23,24</sup> Further study was done on the effect of reductive pulses (0, 50, and 200 pulses) on an ERGO layer deposited with 0.5 mC of total charge (Figure 4b). At a fentanyl concentration of 0.5 ppm, if no pulses were applied, the fentanyl signal increased gradually with each round of oxidation for 1 min and had characteristics of diffusion; however, in both cases with the 50 and 200 pulses, the largest fentanyl signal peak was observed after only one round of pulsing and 1 min of fentanyl oxidation. Pulsing 200 times resulted in a signal approximately twice as large as pulsing 50 times (Figure S6). It appears that pulsing will allow for more sensitive and faster measurements, through beneficial changes in the ERGO layer.

In situ characterization of the pulsed ERGO deposit was performed using EIS. The changes in the ERGO layer after pulsing showed that all the surfaces were affected similarly. The capacitance decreased by 25% for the 0.25 mC layer and 50% for the other two depositions, indicating a loss of material from the surface. The CPE exponent decreased from 0.9 to 0.8, indicating an increase in the porosity of the deposit, although the data did not fit well for the two layers deposited at higher charge. Pulsing had a much larger influence on the 0.5 and 1.0 mC layers. An extra time constant parallel to the CPE was

needed to accurately fit these curves (Figure S1), representing a significant change in the ERGO layer. Introducing an extra time constant into the charging of the interface can be interpreted as a significant increase in porous regions in the ERGO on the electrode. This can be characterized as a RC time constant (1 and 1.7 ms for 0.5 and 1 mC respectively), indicating the charging rate for these porous regions. Pulsing was previously reported to remove the GO overlayer that was deposited electrochemically but not reduced.<sup>23,24</sup> This overlayer on the pre-pulse ERGO deposit appeared to have similar EIS characteristics (the same CPE exponent independent of the deposition time/charge) except for the increased roughness with longer deposition time (Figure S5). The negative potential pulse treatment was proposed to reduce water and create H<sub>2</sub> on the electrically conductive ERGO. This would act to remove the non-conductive overlayer and allow for ingress of the electrolyte into the newly uncovered or newly created porous structures.<sup>23,24</sup> The EIS results are in line with this hypothesis.

A benefit of pulsing and further reduction of the ERGO was that pulsing quickly increased the fentanyl concentration in the ERGO layer. Pulsing increased the rate of ingress of the electrolyte (and fentanyl) into the porous ERGO structure. This strategy of using potential cycling or pulsing is used to improve the wettability of carbon felts or carbon blacks.<sup>25</sup> Additional pulsing and oxidation at +0.8 V up to 4 min decreased the peak current at +0.1 V. This may be a result of the over-oxidation of the ERGO layer, although the decrease was not observed for the no-pulse measurements. More likely, pulsing impacted the diffusion both into and out of the ERGO deposit, resulting in the loss of oxidized fentanyl from the electrode surface with additional pulsing treatment. The major benefit of pulsing an ERGO layer in a solution of fentanyl is an increase in measurement speed and, in this case, only one round of pulsing and subsequent oxidation of fentanyl is required.

**Electrochemical Oxidation of Fentanyl on ERGO.** After having determined the suitable parameters for the construction of an ERGO film on GC, namely, a total charge deposition of 0.5 mC followed by a series of 200 reductive pulses, the surface was rigorously tested for the analysis of fentanyl in PBS. As established in the previous section, fentanyl was oxidized for 1

min at +0.8 V to obtain the largest signal in the shortest period of time.

To ensure a similar behavior on ERGO as on GC, the potential dependence of oxidized fentanyl was measured at discrete potentials in 0.1 V increments from +0.5 to +1 V. The SWV peak at +0.08 V due to redox of the products of fentanyl oxidation measured on ERGO was similar to that of GC, in that the maximum fentanyl signal of 23  $\mu\text{A}$  was obtained at the same potential of +0.8 V (see Figure 5). The large increase in current after a 1 min oxidation at +0.8 V was dramatic at this potential and only observed at +0.7 V but not at other potentials. This behavior was described in the previous section where a series of negative potential pulses likely ensured that the largest amount of fentanyl was in the ERGO film at equilibrium, and additional rounds of pulsing and oxidation appeared to have minimal or perhaps a deleterious effect due to diffusion of the adsorbed species out of the ERGO and/or over-oxidation of the carbon surface.

Under these optimal conditions, a calibration curve for the detection of fentanyl using the SWV peak currents at +0.1 V was generated using an ERGO layer created with a total charge deposition of 0.5 mC (Figure 6). A measurable peak was

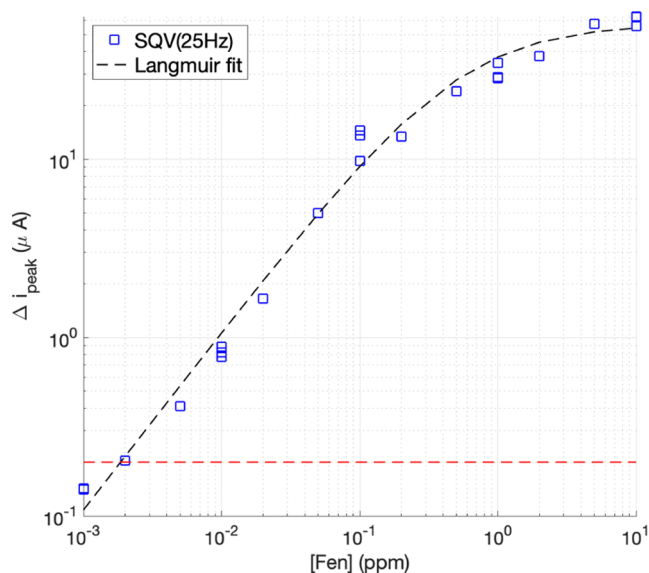


**Figure 6.** Calibration curve for fentanyl detection using an ERGO-modified GC electrode (0.5 mC deposit) based on SWV peak height measured with 25 Hz. Each data point is a separate ERGO layer, subjected to 200 negative potential pulses and 1 min oxidation at +0.8 V/AgAgCl. The curve is from fitting the Langmuir adsorption isotherm with  $\Gamma_{\text{max}} = 55 \pm 5.4 \mu\text{A}$  and  $K_{\text{ads}} = 1.95 \pm 0.25 \text{ ppm}$  ( $r^2 = 0.92$ ). The red line represents the LOQ estimated to be 10 $\times$  the value of the peak height uncertainty ( $0.02 \mu\text{A}$ ) obtained in the analysis of the SQV data for [fentanyl] = 0 and 1 ppb, which was  $0.2 \mu\text{A}$  corresponding to 2 ppb.

recorded over a wide range of concentrations, 1 ppb to 10 ppm in PBS (examples of the SWV scans for each concentration is shown in Figure S7). Importantly, each data point was a separate, independent ERGO layer that was fabricated for the single, one-time oxidation of fentanyl. Fentanyl was detected at the lowest concentration of 1 ppb (or 1  $\mu\text{g}/\text{mL}$ ) with a signal of  $0.15 \pm 0.02 \mu\text{A}$  (error is the uncertainty in the fitted peak height). The SWV measurement of the electrolyte measured in the absence of fentanyl did not detect a measurable peak at +0.1 V with the same uncertainty of  $0.02 \mu\text{A}$ . Therefore, under

these ideal conditions, using the linear range between 1 and 100 ppb in Figure 6, a 2 ppb limit of quantification (LOQ) can be achieved. Given the logarithmic calibration curve, the LOQ was estimated by multiplying the uncertainty in the fitted peak height by 10 $\times$  and determining the [Fen] for this value (represented by the red dashed line in Figure 6).

At higher concentrations (i.e., >1 ppm), the signal becomes attenuated and may be due to the increasing presence and interference due to methanol present in the stock solutions which were used, resulting in concentrations of 0.1% v/v methanol at 1 ppm and increasing to 1% at 10 ppm fentanyl. The adsorption properties of oxidized fentanyl may be sensitive to the hydrophobicity of the electrolyte, which increased with the addition of methanol. This illustrates the challenges that are faced when using this non-specific type of detection. Nevertheless, the calibration curve resembles a Langmuir adsorption isotherm confirmed by a two-parameter fit shown in Figure 6. The linear relationship of CV peak currents on sweep rate measured on GC, and the adsorption isotherm behavior corroborates the adsorption of oxidized fentanyl.

The high sensitivity of the 0.5 mC ERGO layer allowed for the detection of fentanyl to <10 ppb, whereas the lowest a 1 mC ERGO layer or GC could detect was 10 ppb. Replicates were repeated at 1, 10, and 100 ppb and 1 and 10 ppm three times. The poor response of the GC (Figure S8), especially with the roll-off in signal at fentanyl concentrations >1 ppm, highlighted that using ERGO enhanced the performance and sensitivity. Although the thicker 1 mC ERGO layer was not as sensitive as the 0.5 mC ERGO layer (Figure S8), the advantage of a thicker layer is that it can detect fentanyl at higher concentrations without reaching saturation as quickly as the 0.5 mC ERGO layer. Tuning the ERGO modification of the surface for a specific analytical requirement is possible, for example, for higher sensitivity applications such as measuring fentanyl at biologically relevant concentrations using the 0.5 mC ERGO layer or for lower sensitivity applications where a 1 mC ERGO layer could be used in the rapid assessment of drug samples.

The calibration curve showed how replicable the approach is—in particular, since each ERGO layer was created repeatedly—and measuring fentanyl, especially without the need for standard addition or internal standards. By being able to measure fentanyl concentrations equivalent to 3 nM (1 ppb), the approach of using ERGO to enhance sensor sensitivity is sufficient for quantifying fentanyl at biologically relevant concentrations (<80 nM), though further work is required to realize these detection limits in complex biological matrices.<sup>19</sup>

**Detection and SWV Frequency Dependence of Fentanyl and Derivatives.** Arguably, the difficulties in identifying opioids in the drug supply are the rapidly evolving nature of synthetic derivatives and the rapid assessment of the presence and identification of fentanyl and other more potent fentanyl derivatives. As shown earlier, the oxidation of fentanyl results in a signal corresponding to an adsorbed species at +0.08 V. In addition to fentanyl, other derivatives have been tested: norfentanyl (a precursor in the synthesis of fentanyl), carfentanil (a more acutely potent and highly toxic derivative of fentanyl), and alfentanil (another synthetic opioid used for anesthesia). The structures of these compounds are shown in Figure 1.

All fentanyl analogues tested (at 1 ppm) after oxidation at +0.8 V for 1 min displayed a peak in the SWV (25 Hz) around +0.08 V (see Figure 7). Unique electrochemical signatures for

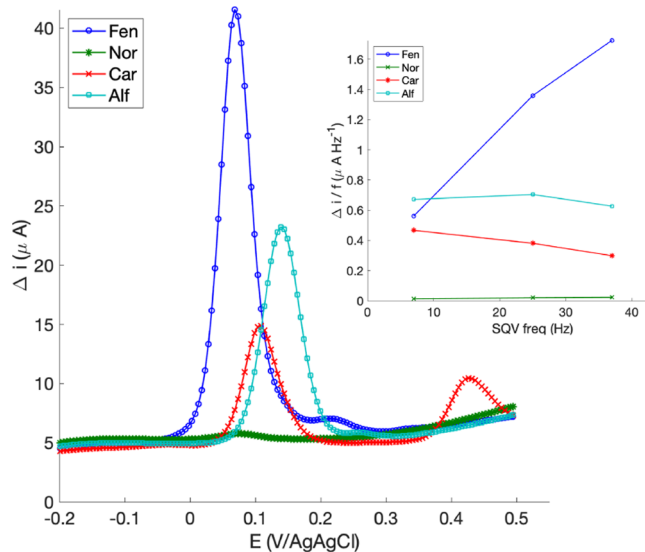


**Figure 7.** SWV scans (positive scans) for four different fentanyl analogues (1 ppm) measured at 25 Hz on a ERGO-modified GC electrode (0.5 mC after 200 negative potential pulses) after 1 min oxidation at +0.8 V/AgAgCl. Inset: Comparison of the frequency-normalized peak currents with SWV frequency for the four fentanyl analogues (Fen—fentanyl, Nor—norfentanyl, Car—carfentanil, and Alf—alfentanil).

each compound were observed and could be used for identification and quantification; for example, alfentanil showed a peak of 18  $\mu\text{A}$  that was the most positive at +0.14 V, whereas carfentanil had a peak of 9  $\mu\text{A}$  at +0.10 V and also produced a secondary peak at +0.42 V that could be useful for measurements of mixtures.

Oxidizing norfentanyl yielded a peak that was centered at the same potential as fentanyl (+0.08 V), although the magnitudes were very different (34  $\mu\text{A}$  for fentanyl compared with 0.5  $\mu\text{A}$  for norfentanyl). In the literature, it is theorized that the adsorbed species formed from fentanyl oxidation is norfentanyl;<sup>19</sup> however, it appeared that the proposed mechanism of oxidation on the ERGO surface was not supported with our data given that there was no evidence of norfentanyl redox from the full SWV scans (Figure S9b) and a very small redox peak after norfentanyl oxidation at +0.8 V. It is possible that +0.8 V is not the optimal oxidation potential for norfentanyl (closer to +1.0 V), but its presence alone does not yield a large signal (as would have been expected had norfentanyl been the redox-active byproduct at +0.1 V as reported previously in the literature). Oxidation of norfentanyl was necessary to produce an adsorbed species with similar electrochemical characteristics as that of oxidized fentanyl. Further study is required to identify the redox-active adsorbed oxidation product of the fentanyl family of compounds.

The fentanyl analogues analyzed differed in the peak potentials measured using SWV and can be advantageous as this property could be used to differentiate between compounds. The peak potentials measured at 25 Hz for the adsorbed oxidized compound differed significantly in some cases (e.g., a +40 mV shift for alfentanil vs fentanyl), which could be exploited for identification. Similarly, the peak

amplitude varied depending on the SWV frequency. As depicted in Figure 7b, all the compounds behaved differently when the SWV measurements were made at 7, 25, and 37 Hz (the SWV are directly compared in Figure S9). The SWV of the adsorbed redox-active species was sensitive to the measurement frequency. The standard rate constant ( $k_s$ ) can be estimated by finding the frequency where  $\Delta i_p/f$  is a maximum.<sup>26,27</sup> Due to the restricted frequency range measured, the data suggest that the redox of the fentanyl oxidation product has a much larger  $k_s$  than the oxidation product for the other analogues.  $\Delta i_p/f$  decreased with frequency for both carfentanil and alfentanil. More study is warranted to investigate the origin of this difference and the oxidation products that are adsorbed. From an analytical point of view, the combination of differing peak potentials in conjunction with the peak current frequency dependence could be used to selectively identify fentanyl and common fentanyl derivatives in a solution using only electrochemical measurements.

**Detecting Fentanyl in the Presence of Other Opiates or Cutting Agents.** The illicit opioid drug supply contains a number of other compounds in addition to the opioid. Often, the sample can contain other psychoactive substances, either unwanted or unknown. In Canada, more than 50% of the accidental deaths involved a stimulant (e.g., cocaine), illustrating the complex nature of the overdose crisis.<sup>1</sup> Presently, the use of fentanyl as an opioid of choice has resulted in a demand for fentanyl. The wide range of fentanyl content in the unregulated drug supply results in many overdose deaths. A quantitative measure of fentanyl in the illicit drug supply would be beneficial for harm reduction strategies, preventing overdose and death.<sup>28,29</sup> We show the advantages of our electrochemical approach of quantifying fentanyl in a drug sample, or as the adulterant in heroin and cocaine samples without having to physically separate fentanyl using a liquid chromatography separation column in an additional step, saving time.

Given that the major oxidative signal for fentanyl, heroin, and cocaine occurs between +0.8 and +1 V (Figure S3), that peak has limited utility in measuring the constituent components from a mixture. As established earlier, the oxidative product of fentanyl and its analogues has an adsorptive peak at +0.08 V and can be used to isolate and measure the fentanyl component of a fentanyl/heroin or fentanyl/cocaine mixture. This was done using a ratio of fentanyl to heroin or fentanyl to cocaine in these experiments, which ranged from 0.1 to 10%. The upper maximum was based on the previous literature, indicating that most drug samples consisted of about 10% fentanyl and overdose deaths revealed an average of about 10% fentanyl to morphine in blood.<sup>30</sup>

Measurements using a mixture of heroin at 10 ppm and fentanyl ranging from 0.01 to 1 ppm (0.1–10%, respectively) were performed. Fentanyl was quantified in the presence of heroin using the adsorption of the oxidized fentanyl (Figure 8). The fentanyl response was attenuated by 40–50% relative to the calibration curve generated in Figure 6, but the response is similar and follows the same trend. A mixture of cocaine at 10 ppm and fentanyl ranging from 10 ppb to 1 ppm also exhibited a comparable behavior (Figure 8) with a similar attenuation in the response. The heroin and cocaine additions were from stock solutions made up in methanol or acetonitrile. The adsorption of the fentanyl oxidation product may be sensitive to the hydrophobic nature of the electrolyte as suggested in the

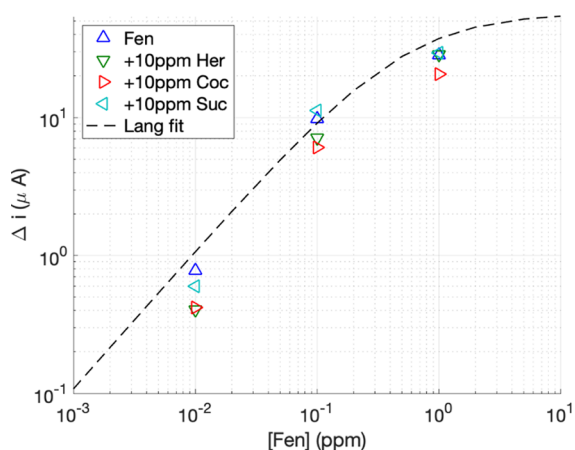


**Figure 8.** Calibration curve for fentanyl detection using an ERGO-modified GC electrode (0.5 mC deposit) based on SWV peak height measured with 25 Hz. Each data point is a separate ERGO layer subjected to 200 negative potential pulses and 1 min oxidation at +0.8 V/AgAgCl. The fitted curve shows the Langmuir adsorption isotherm from Figure 6. Fentanyl was determined in the presence of 10 ppm of heroin (Her), cocaine (Coc), or sucrose (Suc).

calibration curve results (Figure 6). This characteristic points to the need for an internal standard to ameliorate these errors.

By extension, the detection of fentanyl is possible in the presence of other compounds used to bulk-up illicit drug samples, such as sucrose and caffeine; those compounds do not display an electrochemical signal (Figure S10). As illustrated in Figure 8, the presence of sucrose did not significantly affect the fentanyl measurements above 10 ppb. This is important since current methodologies utilize FTIR measurements,<sup>10</sup> which suffer from low sensitivity for fentanyl and the presence of sucrose complicates the quantification of fentanyl. Here, we have established a procedure that enables the in situ detection of fentanyl in the presence of sucrose. FTIR would also struggle with analysis of carfentanil as it would be present in a lower concentration.

In addition, the recent prevalence of benzodiazepines in the illicit drug supply<sup>29</sup> demonstrates that there is a pressing need to be able to detect and quantify both drugs. The fentanyl signal can be separated out from benzodiazepines, such as lorazepam, as it has an oxidative peak around +1.1 V far from the adsorptive peak of fentanyl at +0.08 V.

## CONCLUSIONS

Electroanalysis of fentanyl was demonstrated via the adsorption of the oxidation product of fentanyl, which was used for quantification on GC electrodes. The optimal oxidation potential was determined to be +0.8 V/AgAgCl, resulting in maximum redox peak currents at 0.08 V/AgAgCl when measured by SWV at 25 Hz. Improved detection limits were achieved with an ERGO modification of the GC electrode. This created a large surface area and a porous electrode surface, which enhanced the detection limit of the adsorbed oxidation product of fentanyl. The ERGO deposition conditions could be modified to optimize the deposit (thick or thin) tailored to the analytical requirements of greater sensitivity or a larger working range. Before analytical measurements, a pre-treatment using reductive potential pulsing was found to quickly exchange the electrolyte within the extended (three-dimensional) electrode volume, reducing the time for analysis. The LOQ was estimated to be  $\leq 10$  ppb

under optimal conditions in PBS using SWV. Fentanyl analogues such as carfentanil and alfentanil were also detected using the same method but at differing levels of sensitivity. Differences in the redox potential and the frequency dependence of the SWV peak currents were observed, which provide an opportunity for detection of a mixture of fentanyl-like compounds using this method. Norfentanyl did not produce a significant redox peak under these conditions, suggesting that it is not the adsorbed product of fentanyl oxidation that was used for quantification. Fentanyl detection via the adsorption of oxidized fentanyl produced similar results in the presence of a 100-fold excess of other compounds that may be found in illicit drug samples such as heroin, cocaine, caffeine, or sucrose. This measurement strategy provides a platform for the development of an inexpensive and sensitive POU device for drug checking services, which form part of the harm mitigation strategies used in response to the opioid overdose crisis.

## ASSOCIATED CONTENT

### Supporting Information

The Supporting Information is available free of charge at <https://pubs.acs.org/doi/10.1021/acs.analchem.2c02057>.

Equivalent circuits used for EIS analysis; example GO electrodeposition current and charge transients; SWV positive potential scans for fentanyl analogues (fentanyl, norfentanyl, carfentanil, and alfentanil) on GC; CV sweep rate analysis of the redox characteristics of the adsorbed product of fentanyl oxidation; EIS analysis for the ERGO-modified GC electrode for three different deposition conditions; SWV (25 Hz) peak heights of the adsorbed fentanyl oxidation product for three ERGO layers studied; SWV positive potential scans used for the calibration curve for fentanyl detection; calibration curve for fentanyl detection on an unmodified GC electrode and ERGO-modified GC electrode SWV scans (positive potential sweep) for four fentanyl analogues (fentanyl, norfentanyl, carfentanil, and alfentanil) measured using 7, 25, and 37 Hz. SWV positive potential scans for nine compounds of interest performed at different frequencies on GC. Examples of EIS fitting results after GO deposition (post-deposition) and after negative pulse treatment (post-pulse) (PDF)

## AUTHOR INFORMATION

### Corresponding Author

**Dan Bizzotto** – AMPEL, University of British Columbia, Vancouver V6T1Z4, Canada; Department of Chemistry, University of British Columbia, Vancouver V6T1Z1, Canada; [orcid.org/0000-0002-2176-6799](https://orcid.org/0000-0002-2176-6799); Email: [bizzotto@chem.ubc.ca](mailto:bizzotto@chem.ubc.ca)

### Authors

**Daniel Jun** – AMPEL, University of British Columbia, Vancouver V6T1Z4, Canada; Department of Chemistry, University of British Columbia, Vancouver V6T1Z1, Canada  
**Glenn Sammis** – Department of Chemistry, University of British Columbia, Vancouver V6T1Z1, Canada; [orcid.org/0000-0002-8204-8571](https://orcid.org/0000-0002-8204-8571)  
**Pouya Rezazadeh-Azar** – Complex Pain and Addiction Services, Department of Psychiatry, Vancouver General Hospital, Vancouver V5Z 1M9, Canada; Department of



Psychiatry, University of British Columbia, Vancouver  
V6T2A1, Canada

Erwann Ginoux – AMPEL, University of British Columbia,  
Vancouver V6T1Z4, Canada

Complete contact information is available at:

<https://pubs.acs.org/10.1021/acs.analchem.2c02057>

## Notes

The authors declare no competing financial interest.

## ACKNOWLEDGMENTS

This work was supported by VGH foundation (Innovators Challenge Award) and MITACs Accelerate grant for D.J., with initial seed funding provided by UBC UILO. The authors acknowledge the support of Dr. Martha J. Ignaszewski (VGH), George P. Budd (VGH), James Wong (VGH), Robert Bush (VGH), and Dr. JJ Sidhu (VGH).

## REFERENCES

- (1) Special Advisory Committee on the Epidemic of Opioid Overdoses. Opioid- and Stimulant-related Harms in Canada, Ottawa. <https://health-infobase.canada.ca/substance-related-harms/opioids-stimulants>, (accessed June 01, 2022).
- (2) Harm Reduction International. *Global State of Harm Reduction 2020*, 7th ed.; Harm Reduction International: London, 2020.
- (3) Galarneau, L. R.; et al. *PLoS One* **2021**, *16*, No. e0255396.
- (4) Burns, S. M.; Cunningham, C. W.; Mercer, S. L. *ACS Chem. Neurosci.* **2018**, *9*, 2428–2437.
- (5) Ringuette, A. E.; Spock, M.; Lindsley, C. W.; Bender, A. M. *ACS Chem. Neurosci.* **2020**, *11*, 3955–3967.
- (6) Sordo, L.; Barrio, G.; Bravo, M. J.; Indave, B. I.; Degenhardt, L.; Wiessing, L.; Ferri, M.; Pastor-Barriuso, R. *BMJ* **2017**, *357*, j1550.
- (7) Busardó, F. P.; Carlier, J.; Giorgetti, R.; Tagliabracchi, A.; Pacifici, R.; Gottardi, M.; Pichini, S. *Front. Chem.* **2019**, *7*, 184.
- (8) Kang, M.; Lian, R.; Zhang, X.; Li, Y.; Zhang, Y.; Zhang, Y.; Zhang, W.; Ouyang, Z. *Talanta* **2020**, *217*, 121057.
- (9) Purohit, S.; Pandey, G.; Tharmavaram, M.; Rawtani, D.; Mustansar Hussain, C. M. *Sensors for the Detection of Illicit Drugs. Technology in Forensic Science*; John Wiley & Sons, Ltd, 2020; pp 221–238.
- (10) Ti, L.; Tobias, S.; Lysyshyn, M.; Laing, R.; Nosova, E.; Choi, J.; Arredondo, J.; McCrae, K.; Tupper, K.; Wood, E. *Drug Alcohol Depend.* **2020**, *212*, 108006.
- (11) Achilli, G.; Cellerino, G. P.; Melzi d'Eril, G. V. M.; Tagliaro, F. *J. Chromatogr. A* **1996**, *729*, 273–277.
- (12) Honeychurch, K. *Separations* **2016**, *3*, 28.
- (13) Schwartz, R. S.; David, K. O. *Anal. Chem.* **2002**, *57*, 1362–1366.
- (14) Zangrogini, B.; Pigani, L.; Zanardi, C. *J. Solid State Electrochem.* **2020**, *24*, 2603–2616.
- (15) Moonla, C.; Goud, K. Y.; Teymourian, H.; Tangkuaram, T.; Ingrande, J.; Suresh, P.; Wang, J. *Talanta* **2020**, *218*, 121205.
- (16) Mishra, R. K.; Goud, K. Y.; Li, Z.; Moonla, C.; Mohamed, M. A.; Tehrani, F.; Teymourian, H.; Wang, J. *J. Am. Chem. Soc.* **2020**, *142*, 5991–5995.
- (17) Ott, C. E.; Cunha-Silva, H.; Kuberski, S. L.; Cox, J. A.; Arcos-Martínez, M. J.; Arroyo-Mora, L. E. *J. Electroanal. Chem.* **2020**, *873*, 114425.
- (18) Goodchild, S. A.; Hubble, L. J.; Mishra, R. K.; Li, Z.; Goud, K. Y.; Barfidokht, A.; Shah, R.; Bagot, K. S.; McIntosh, A. J. S.; Wang, J. *Anal. Chem.* **2019**, *91*, 3747–3753.
- (19) Glasscott, M. W.; Vannoy, K. J.; Iresh Fernando, P. U. A. I.; Kosgei, G. K.; Moores, L. C.; Dick, J. E. *TrAC, Trends Anal. Chem.* **2020**, *132*, 116037.
- (20) Sohoulí, E.; Keihan, A. H.; Shahdost-fard, F.; Naghian, E.; Plonska-Brzezinska, M. E.; Rahimi-Nasrabadi, M.; Ahmadi, F. *Mater. Sci. Eng., C* **2020**, *110*, 110684.
- (21) Wester, N.; Mynttinen, E.; Etula, J.; Lilius, T.; Kalso, E.; Mikkladal, B. F.; Zhang, Q.; Jiang, H.; Sainio, S.; Nordlund, D.; Kauppinen, E. I.; Laurila, T.; Koskinen, J. *ACS Appl. Nano Mater.* **2020**, *3*, 1203–1212.
- (22) Lasia, A. *Electrochemical Impedance Spectroscopy and its Applications*; Springer: New York, 2014.
- (23) Li, Y.; Martens, I.; Cheung, K. C.; Bizzotto, D. *Electrochim. Acta* **2019**, *319*, 649–656.
- (24) Liu, Z.; Grzędowski, A. J.; Guo, Y.; Bizzotto, D. *J. Electrochem. Soc.* **2021**, *168*, 096507.
- (25) Li, M.; Idros, M. N.; Wu, Y.; Burdyny, T.; Garg, S.; Zhao, X. S.; Wang, G.; Rufford, T. E. *J. Mater. Chem. A* **2021**, *9*, 19369–19409.
- (26) Komorsky-Lovrić, Š.; Lovrić, M. *Anal. Chim. Acta* **1995**, *305*, 248–255.
- (27) Komorsky-Lovrić, Š.; Lovrić, M. *J. Electroanal. Chem.* **1995**, *384*, 115–122.
- (28) Long, V.; Arredondo, J.; Ti, L.; Grant, C.; DeBeck, K.; Milloy, M. J.; Lysyshyn, M.; Wood, E.; Kerr, T.; Hayashi, K. *Harm Reduct. J.* **2020**, *17*, 100.
- (29) Scarfone, K. M.; Maghsoudi, N.; McDonald, K.; Stefan, C.; Beriault, D. R.; Wong, E.; Evert, M.; Hopkins, S.; Leslie, P.; Watson, T. M.; Werb, D.; Group, T. D. C. S. W. *Harm Reduct. J.* **2022**, *19*, 3.
- (30) Hwang, C. S.; Smith, L. C.; Natori, Y.; Ellis, B.; Zhou, B.; Janda, K. D. *ACS Omega* **2018**, *3*, 11537–11543.

## Recommended by ACS

### Potentiodynamic Poly(resorcinol)-Modified Glassy Carbon Electrode as a Voltammetric Sensor for Determining Cephalexin and Cefadroxil Simultaneously in Pharmaceut...

Adane Kassa, Atakilt Abebe, *et al.*

SEPTEMBER 14, 2022  
ACS OMEGA

READ 

### Flow Injection Amperometric Measurement of Formalin in Seafood

Kamonchanok Torrarit, Warakorn Limbut, *et al.*

MAY 18, 2022  
ACS OMEGA

READ 

### Reagentless Voltammetric Identification of Cocaine from Complex Powders

Kathryn J. Vannoy, Jeffrey E. Dick, *et al.*

SEPTEMBER 06, 2022  
ANALYTICAL CHEMISTRY

READ 

### Laser-scribed Graphene Electrodes Functionalized with Nafion/Fe<sub>3</sub>O<sub>4</sub> Nanohybrids for the Ultrasensitive Detection of Neurotoxin Drug Cloiquinol

Rajesh Madhuvilakku, Guang-Wei Huang, *et al.*

APRIL 29, 2022  
ACS OMEGA

READ 

Get More Suggestions >